

Computation of the Basins of Attraction in Non-smooth Dynamical Systems

Ugo Galvanetto and Alessandro Colombo

Abstract The paper discusses several issues related to the numerical computation of the stable manifold of saddle-like periodic cycles in piecewise smooth dynamical systems. Results are presented for a particular stick–slip system. In the second part of the paper the same mechanical model is used to briefly describe the interaction between fold and adding-sliding bifurcations.

Keywords Non-smooth dynamical systems • Stable manifolds • Computational methods

1 Introduction

Engineering systems affected by some form of nonlinearity can exhibit multiple stable solutions under steady state conditions of the external forces. If the system is dynamic it is common to express this concept by saying that there are coexisting attractors. Usually only one of them represents the normal working mode of the system from an engineering point of view, whereas the others are conditions to be avoided because the system is too deformed or cannot function (safely) if it reaches them. A classical problem of engineering mechanics is to determine whether the normal working mode of the system is robust with respect to perturbations. These can often be represented as variations in the positions or the velocities of the system.

U. Galvanetto (✉)

Department of Structural and Transportation Engineering, University of Padua,
35131 Padova, Italy
e-mail: ugo.galvanetto@unipd.it

A. Colombo

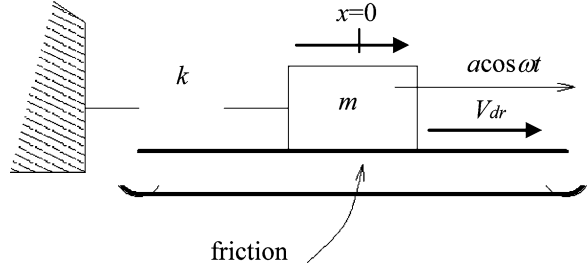
Department of Electronics and Information, Politecnico di Milano, 22100 Como, Italy
e-mail: alessandro.colombo@polimi.it

They are acceptable as long as they do not bring the system far from its normal working mode, or unacceptable otherwise. In simple smooth systems, it is possible to adopt a new design approach aiming at defining, within the basin of attraction, a “safety set” of all initial conditions which do not compromise the integrity of the system (Cruck et al. 2001; Barreiro et al. 2002). In these cases, the overall size of the basin can provide a measure of the safety or robustness of an engineering system. Another measure could be provided by the distance between the attractor and its basin’s boundaries, that would provide an indication of the size or the duration of the perturbation needed to bring the system out of the safety basin. Since engineering systems may be subjected to pulse loads of finite duration, attention should be given to both the absolute basins, related to steady external forcings, and transient basins corresponding to transient excitations. Similar ideas have been proposed in the past, for example in (Soliman and Thompson 1989; Thompson and Soliman 1990). Therefore one of the classical problems in nonlinear dynamics, the computation of the basins boundaries, which separate safe initial conditions from the unsafe ones, could in the future become a standard step in the design of systems of engineering relevance. In particular in smooth dynamical systems the boundaries of the basins of attraction of coexisting attractors consist of stable manifolds of saddle limit sets. The numerical computation of invariant manifolds has interested several researchers in the past (Parker and Chua 1989) and has been practically solved for the case of smooth dynamical systems. In the present work some properties of the stable manifolds of equilibria or cycles of saddle type are discussed for the case of piecewise smooth dynamical systems (Galvanetto 2008; Colombo and Galvanetto 2009). Our results can in principle be applied to systems of any dimension, but the details reported here concern in particular three-dimensional systems, where the computation of invariant manifold is of practical use and it is easier to visualize the concepts. In particular, a crucial ingredient for the application of the method is the understanding of the geometric constraints that the piecewise nature of the flow imposes on the shape of the manifold (Colombo and Galvanetto 2009). The final part of the paper presents a few results regarding transitions and bifurcations of the piecewise smooth steady state motions investigated in earlier sections of the paper.

2 The Forced Friction Oscillator

The non-smooth dynamics investigated in the present work is generated by the system sketched in Fig. 1, that was presented in reference (Oestreich et al. 1996): a block of mass m is supported by a belt moving with constant velocity V_{dr} . The block is connected to a fixed support by a linear elastic spring of stiffness k , which assumes its unstretched length for $x = 0$, and is subjected to an external harmonic force of magnitude a and frequency ω . While the block rides on the belt with no relative motion between them, the motion is in a stick phase described by the two states of the system position x and time t in the following equation:

Fig. 1 The mechanical model under investigation



$$x(t) = x(t_0) + V_{dr}(t - t_0) \quad (1)$$

where $x(t_0)$ is the position of the block at time $t = t_0$. The block can stick if $\dot{x} = V_{dr}$ and the following conditions are simultaneously true:

$$-\frac{F_{sf}}{k} + \frac{a}{k} \cos \omega t \leq x \quad (2a)$$

$$x \leq \frac{a}{k} \cos \omega t + \frac{F_{sf}}{k} \quad (2b)$$

where F_{sf} is the magnitude of the maximum static friction force. The two sinusoidal functions of time $x(t) = [(a/k) \cos \omega t \pm F_{sf}/k]$ are the boundaries in the plane (x, t) of the stick zone. Once either of the two inequalities (2) is satisfied as equality an accelerated motion starts, called slip phase, which can be of two types:

$$\text{forward slip phase} \quad m\ddot{x} + kx = a \cos \omega t - F_{kf}, \quad \text{if } \dot{x} > V_{dr} \quad (3a)$$

$$\text{backward slip phase} \quad m\ddot{x} + kx = a \cos \omega t + F_{kf}, \quad \text{if } \dot{x} < V_{dr} \quad (3b)$$

where F_{kf} is the magnitude of the kinetic friction force which will be defined later. The motion described by Eq. (3a) starts when the equality in (2a) is verified, and the speed of the block is greater than V_{dr} ; otherwise if the equality in (2b) is verified then the dynamics given by Eq. (3b) starts, and the speed of the block is less than V_{dr} . During a slip phase the system is described by three states, x , t and velocity \dot{x} .

The static friction force can assume any value in the range between $-F_{sf} = -\mu_s mg$ and $F_{sf} = \mu_s mg$; where $\mu_s (= \alpha + \beta)$ is the coefficient of static friction and mg is the weight of the block. The magnitude of the kinetic friction force is a function of the relative velocity and is defined as $F_{kf} = \mu_k mg$, where μ_k is the coefficient of kinetic friction defined as (Fig. 2):

$$\mu_k = \frac{\alpha}{1 + \gamma |\dot{x} - V_{dr}|} + \beta + \eta (\dot{x} - V_{dr})^2 \quad (4)$$

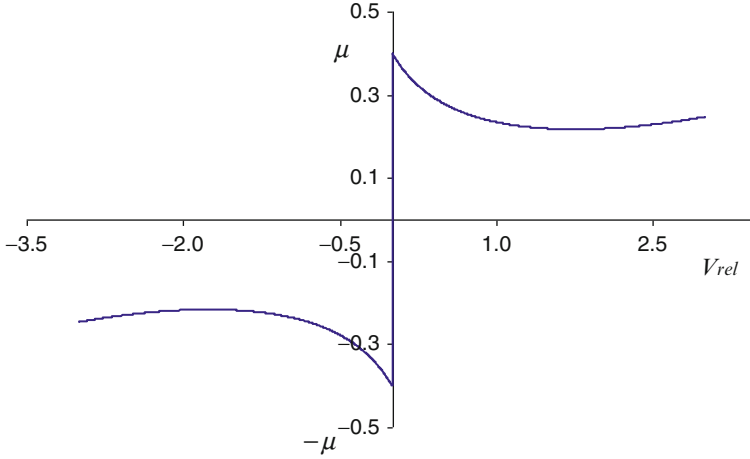


Fig. 2 Example of a commonly adopted friction characteristic, $V_{rel} = V_{dr} - \dot{x}$

If during an accelerated motion governed by either of Eqs. (3) the velocity of the block coincides with that of the belt and the position of the block is within the boundaries of the sticking region, then the block sticks to the belt and its motion is described again by Eq. (1) in which t_0 is the instant of re-attachment.

In the formalism usually adopted in the literature on non-smooth dynamical systems (Di Bernardo et al. 2007) Eqs. (3), written in a way familiar to most engineers, are recast in the following form:

$$\dot{x} = f(x) = \begin{cases} f_1(x) & \text{if } h(x) > 0 \\ f_2(x) & \text{if } h(x) < 0 \end{cases} \quad (5)$$

Where $x = (x_1, x_2) = (x, \dot{x})$, $h(x) = x_2 - V_{dr}$ and

$$f_1(x) = \begin{cases} \frac{-kx_1 + a \cos(\omega t)}{m} - g \left(\frac{x_2}{1 + \gamma(x_2 - V_{dr})} + \beta + \eta(x_2 - V_{dr})^2 \right) \end{cases} \quad (6a)$$

$$f_2(x) = \begin{cases} \frac{-kx_1 + a \cos(\omega t)}{m} + g \left(\frac{x_2}{1 - \gamma(x_2 - V_{dr})} + \beta + \eta(x_2 - V_{dr})^2 \right) \end{cases} \quad (6b)$$

In the paper the parameter values are fixed:

$$\begin{array}{llllll} m = 1 & k = 1 & a = 3.5 & \omega = 1.0 & g = 10 & V_{dr} = 1 \\ \alpha = 0.3 & & \beta = 0.1 & \mu_s = 0.4 & \gamma = 1.42 & \eta = 0.01 \end{array}$$

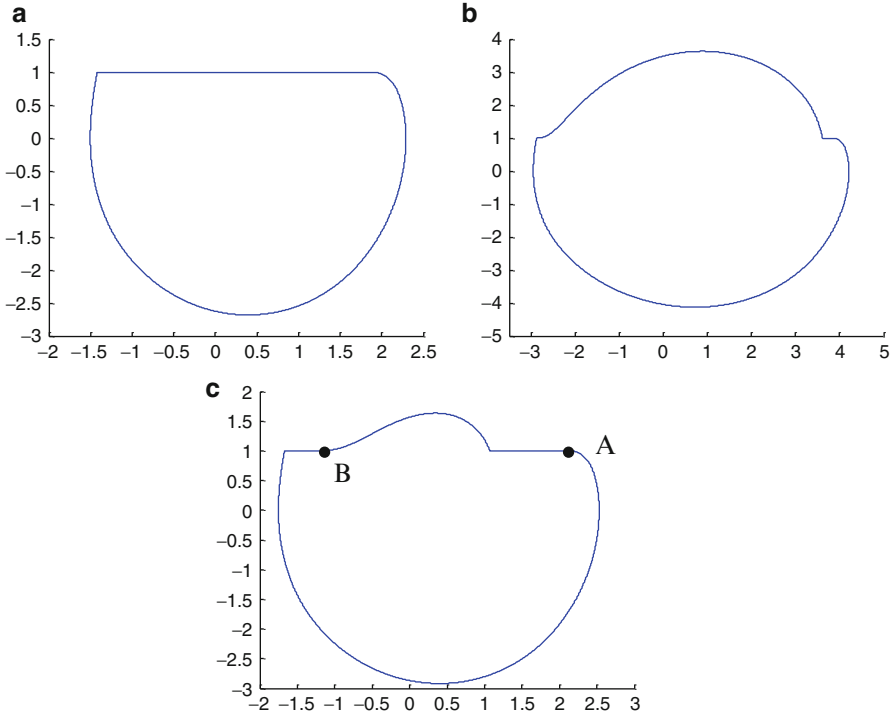


Fig. 3 (a) motion-1s, (b) motion-2s, (c) motion-2u. The scales of the figures are not the same

The friction characteristic adopted is the same presented in (Oestreich et al. 1996) and is considered a good approximation of physically observed friction behaviours.

The mechanical system under investigation with the above parameter values posses (at least) three steady states: two attractors and a saddle cycle as shown in Fig. 3. The nature of the stability of the steady states and the algorithms adopted to accurately locate unstable stick–slip motions have been described elsewhere (Galvanetto 2000, 1999). The three steady states are called motion-1s, motion-2s and motion-2u where the numbers 1 or 2 indicate how many stick phases are present and the letter s or u indicate respectively the stable or unstable nature of the steady state. In the plane of initial conditions (x, \dot{x}) at time zero the stable manifold of the saddle cycle forms the boundary between the basins of the two coexisting attractors. Figure 4 shows the basin of motion-2s (and of motion-1s) computed with a cell-mapping type algorithm (Hsu 1987).

In Fig. 3c the saddle cycle of a stick–slip system is characterised by two portions of sticking branch, the horizontal segments; points A and B on the orbit indicate where the stick–slip transitions take place: the stick–slip transitions appear smoother than the slip–stick transitions, this fact is related with the degree of continuity in the friction force. If $\dot{x} = V_{dr}$ in Eq. (4) then $\mu_s = \mu_k = \alpha + \beta$ therefore the transition

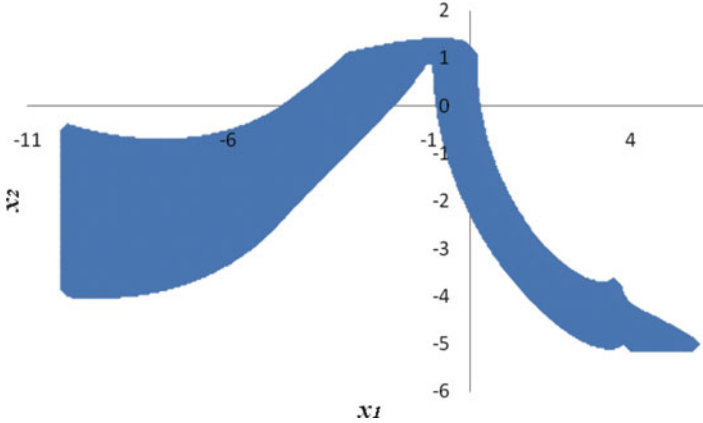


Fig. 4 The blue area is the basin of attraction of motion-2s in the window $-10 < x < 5$, $-5 < \dot{x} < 2$

from the static friction force to the kinetic friction force is continuous, although it is non smooth as shown in Fig. 2. Vice versa the transition between kinetic and static friction is in general associated to a jump in the forces applied to the block and therefore in its acceleration (Galvanetto 1999). At a transition from kinetic to static friction the friction force usually jumps from one of the two the extreme values $\pm(\alpha + \beta)mg$ to a value within the range $-(\alpha + \beta)mg \div +(\alpha + \beta)mg$ defined by the following equilibrium equation:

$$F_s = kx - a \cos \omega t$$

in which the value of x is that of the slip–stick transition provided by the numerical integration.

3 Reconstruction of the Stable Manifold

Figure 5 is a sketch of the flow around any of the two sticking branches of motion-2u: if $\dot{x} > V_{dr}$ the trajectories intersect transversally the line $\dot{x} = V_{dr}$ from above; in a similar way in the half-plane $\dot{x} < V_{dr}$ the trajectories intersect transversally the line $\dot{x} = V_{dr}$ from below. Every point of the sticking phase can be thought to belong simultaneously to three trajectories: the sticking-trajectory, the trajectory converging to it from above and the trajectory converging from below. The main idea of the method proposed in (Galvanetto 2008; Colombo and Galvanetto 2009) to compute the stable manifold of a saddle cycle, is that the stable manifold can be numerically reconstructed by integrating backwards in time all trajectories that in forward time converge to the saddle limit set, thus, in the case of the cycle in Fig. 3c,

Fig. 5 Sketch of the flow near a sticking branch

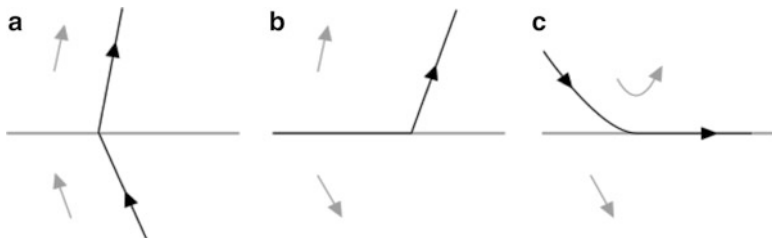
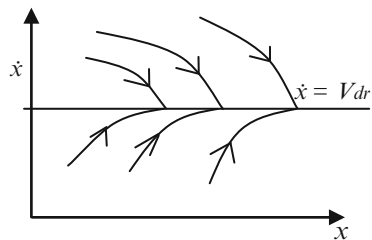


Fig. 6 Geometry of a single trajectory on the stable manifold at a generic intersection with a discontinuity surface. In the figure, *arrows* on the orbits indicate the positive direction of time, while *grey arrows* sketch the vector field above and below the switching surface

all trajectories that converge to the sticking branches of the cycle. Once a single trajectory of the stable manifold is found, the whole manifold can be constructed by numerical continuation, following the trajectory as its end point is changed along the manifold. This idea has been successfully used in smooth systems and is explained for example in (Krauskopf et al. 2005). To apply it to a piecewise smooth dynamical system, a first and fundamental step is to understand how the orbits, and the families of orbits that constitute a stable manifold, intersect the surfaces of discontinuity of the system, taking into account the non-reversibility introduced by the non-smooth nature of the flow. A careful look at the generic geometries of intersection of families of orbits with smooth discontinuity surfaces, casted into the framework of singularity theory, allows to conclude that a generic orbit belonging to a stable manifold intersects a discontinuity boundary in one of the three scenarios in Fig. 6, while a one-parameter family of orbits, that is, a two dimensional stable manifold, may contain some of the seven singular points depicted in Fig. 7. Additionally, certain conditions that have been identified, give place to some more singular points, analogous to the one in Fig. 7g, where however the complex interplay of vector fields with the discontinuity boundary cause a breakup of the manifold. The geometries and consequences of these cases are subject of ongoing research. Although, as shown in this short discussion, the geometry of these manifold can be rather intricate, the picture is, in most applications, quite simpler.

As long as all sticking branches are stable, meaning that slipping trajectories converge to the branch, rather than diverging, only scenarios (b) and (e) in Fig. 7 are possible, since all others include unstable sticking branches. Many mechanical and engineering systems admit only stable sticking phases, and in these cases scenarios

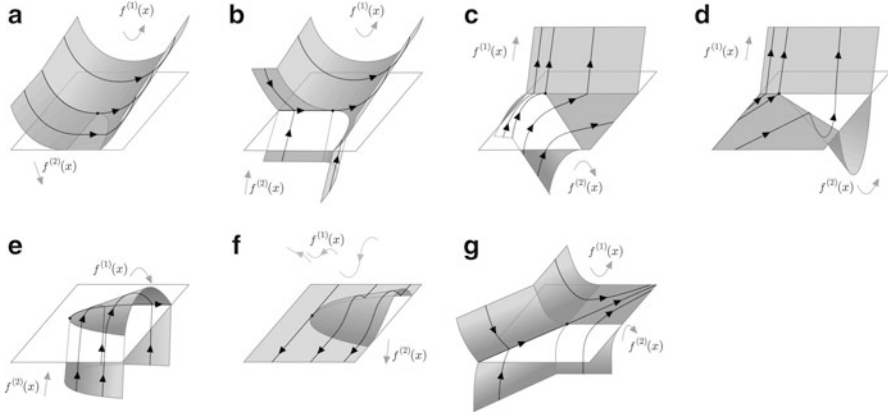


Fig. 7 Geometry of the stable manifold around each one of the seven singular points, [7]

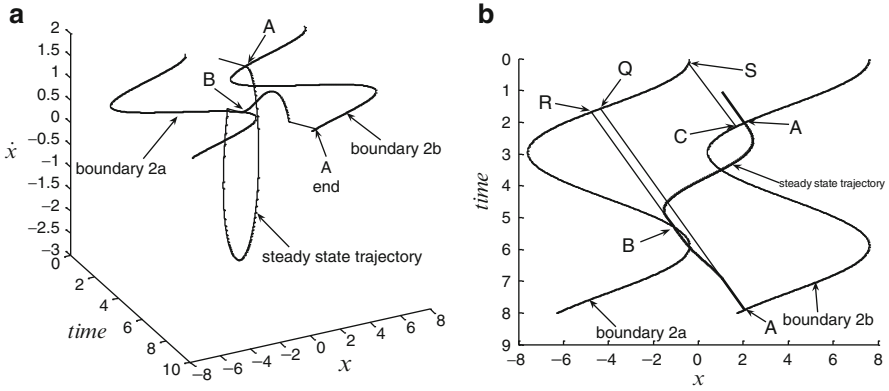
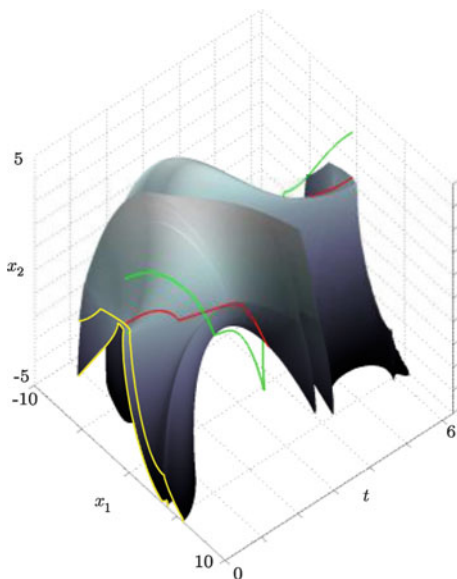


Fig. 8 (a) Three-dimensional phase portrait; the *thick line* is the trajectory of the unstable steady state and the *thin lines* are the boundaries of the stick zone. (b) Projection of figure (a) on the plane displacement-time; [6]

(b) and (e) are sufficient for the analysis (as long as the stable manifold is two-dimensional). They represent respectively the end and start points of a sticking phase.

Figure 8a is a three-dimensional view of the unstable limit cycle of Fig. 3c in its phase space. Thick lines indicate the steady states, thin sinusoidal lines in the plane (x, V_{dr}, t) show the boundaries of the stick zone. Since the saddle cycle has (two) sticking segments, all orbits of its stable manifold must eventually converge to these segments, each one of which can therefore be chosen as the family of end points to generate the whole manifold. The stick phase ending at point A required by the new method, is not only the portion belonging to the steady state trajectory shown in Fig. 8a; it is the whole stick phase shown by the thin straight line AQ in Fig. 8b, since it is apparent that all points belonging to such line will be attracted to the unstable limit cycle. The stick phase AQ is found by starting from the end point

Fig. 9 Stable manifold of motion-2u; the *green lines* represent attractors and the *red line* the saddle-cycle. The *yellow lines* are the basin boundary to be compared with that of Fig. 4



A and integrating backward in time along the stick trajectory to the first intersection (point Q) with one of the boundaries of the stick phase. The same concept applies to the other stick phase ending at B . The two portions of straight lines AQ and BR are stick phases partially belonging to the unstable limit cycle and partially attracted by it. They are not necessarily all the stick phases attracted by the unstable limit cycle, transient stick phases could exist (and do exist!) which generate slip trajectories eventually attracted by motion-2u. Infinitely many of these transient stick phases could exist, as shown in (Galvanetto 2008). In the example examined in the present paper only one transient stick-phase exists, which is indicated by the line CS in Fig. 8b.

In Fig. 8b a transient slip trajectory could be drawn to connect point C with a point of the line AQ , but it is not shown for clarity reasons. Points A, B, C of Fig. 8 are singular points of the stable manifold of the type shown in Fig. 7b, whereas points R, Q, S are singular points such as the one sketched in Fig. 7e. It is worth observing that the knowledge of only one of the stick phases (for example AQ) is sufficient to reconstruct computationally the whole manifold, since all others stick phases are connected to it, either backward or forward in time. The algorithm adopted for the computation of the stable manifold is fully described elsewhere (Colombo and Galvanetto 2009).

Figure 9 shows part of the non-smooth stable manifold computed with the method presented above. All orbits that, departing from the saddle cycle backward in time, remain between the surfaces $|\dot{x}| > 5$, are represented. The intersection of the manifold with the plane $t = 0$ is marked in yellow, and corresponds to the boundary of the basin shown in Fig. 4. Moreover Fig. 10 shows two projections of the same manifold on the planes $\dot{x} = 0$ and $x = 0$.

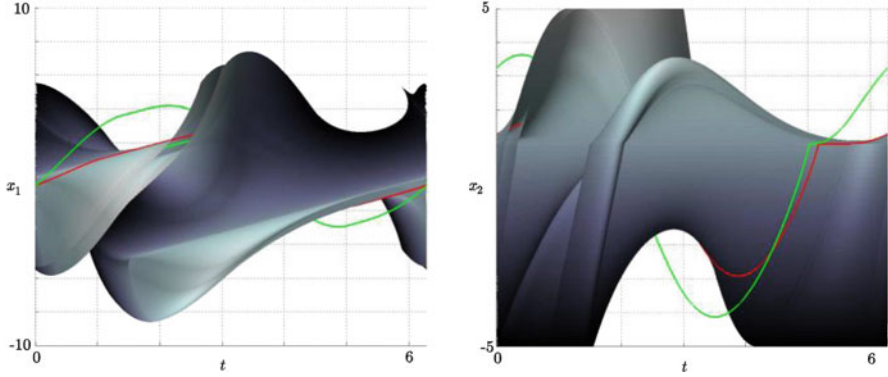


Fig. 10 Projections of the stable manifold on the planes $\dot{x} = 0$, left, and $x = 0$, right. Green orbits are attractors, the red orbit is the saddle cycle

4 Remarks on Transitions and Bifurcations

In this last section of the paper we briefly describe how bifurcations and transitions can interact in the evolution of the dynamics as a parameter is changed. For the given set of parameter values there exist three steady state motions: motion-1s, motion-2s and motion-2u, as already explained above. In reference (Merillas 2006) a smooth co-dimension-two cusp bifurcation was presented. As can be seen in Fig. 11, taken from the same reference, from the cusp point B_2 , two branches of fold bifurcation, which we shall denote by Γ_{f1} and Γ_{f2} , merge (tangentially). The resulting wedge divides the parameter plane into two regions. In region 1, inside the wedge, there are the three solutions shown in Fig. 3, while in the other region, outside the wedge, there is a single solution, which is stable. Varying ω and crossing either Γ_{f1} or Γ_{f2} away from the cusp point we find a non-degenerate fold bifurcation. Along a third bifurcation curve (not depicted in Fig. 11) inside the wedge, motion-1s gains one more sticking segment, becoming topologically equivalent to motion-2u. This is known in the literature as adding sliding bifurcation (Di Bernardo et al. 2007).

These bifurcations might be better understood by looking at the 1-d map induced by the system, see (Oestreich et al. 1996) on how to obtain the map, which shows some features of the dynamics of the system itself. Motion-1s has only one stick phase, motion-2s and motion-2u have two stick phases, for that reason motion-1s can be seen in the first-iterated map and in the second-iterated map as a fixed point of the map. Motion-2s and motion-2u can only be seen as fixed points of the second-iterated map shown in Fig. 12.

If the force frequency is reduced to $\omega = 0.95$ only motion-2s survives, as shown in Fig. 13a. Motion-1s and motion-2u do not exist because there is no intersection between the map and the bisection line at 45° . The sudden disappearance of motion-1s can be understood looking at the second iterated map of Fig. 13a, b.

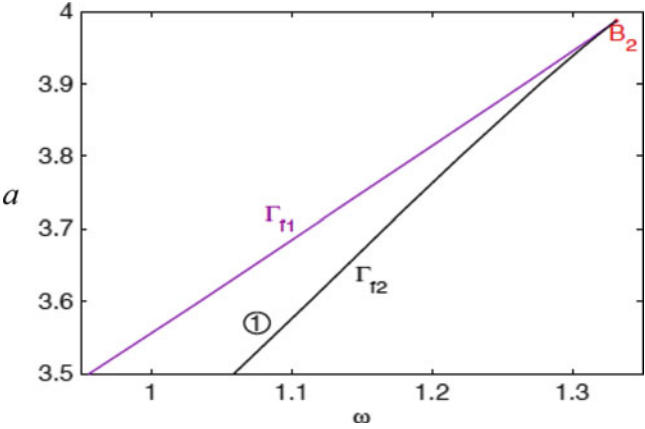
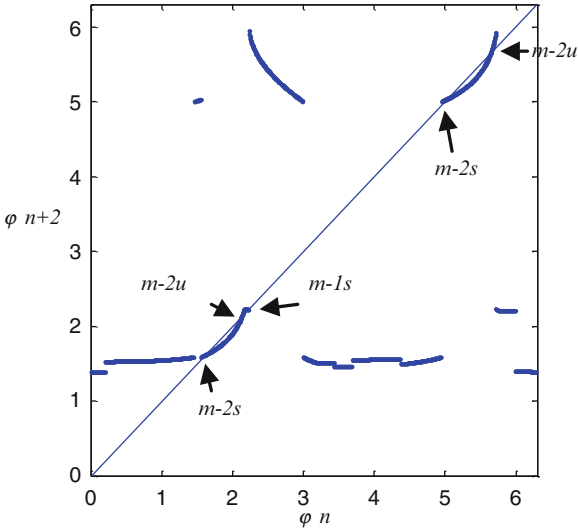


Fig. 11 Bifurcation diagram taken from page 99 of Merillas (2006)

Fig. 12 Second iterated map showing motion-1s, motion-2s and motion-2u for $\omega = 1$



Motion-1s and motion-2u have collided in what appears to be a non-degenerate fold bifurcation which takes place after a transition has affected motion-1s: before the fold occurs the trajectory of motion-1s changes so that a second branch of stick phase appears. Once the transition has taken place the fold involves two motions with the same topological structure. Figure 13b shows the second-iterated map for an intermediate value of the parameter ω for which all three steady states are characterized by two stick phases. Summarizing: for the parameter values defined above the system possess the three steady states shown in Fig. 3. If the value of the parameter ω is reduced below 1, an adding-sliding bifurcations adds a stick phase to motion-1s, which is then shown in Fig. 13b as motion-1sa and -1sb. A further

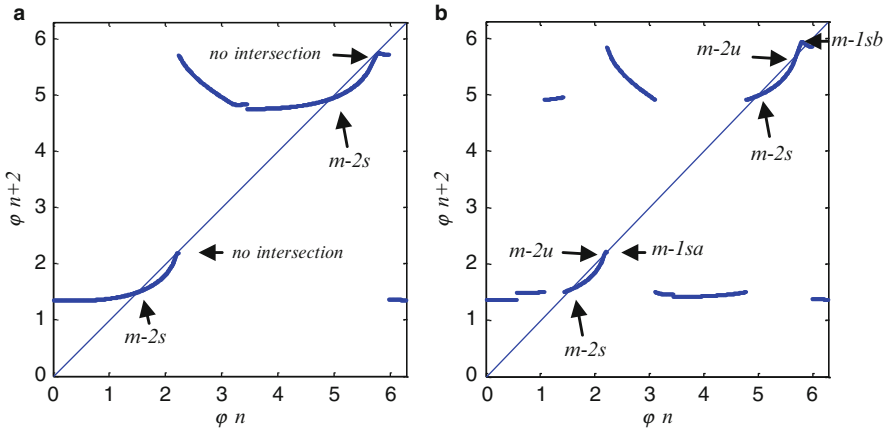


Fig. 13 (a) $\omega = 0.95$: second iterated map showing only one, period-2 motion for the map, corresponding to motion-2s. (b) $\omega = 0.975$: second iterated map showing three period-2 steady states for the map corresponding to motion-2u, motion-2s, and the motion generated at the adding-sliding bifurcation from motion-1s

reduction of ω causes a standard fold bifurcation in which motion-2u disappears colliding with motion-1s. Several adding-sliding bifurcation lines exist in the wedge of Fig. 11.

5 Conclusions

The paper presents the main ideas of a method to compute the stable manifolds of saddle-like periodic cycles in piece-wise smooth dynamical systems. They represent the basin boundaries of the relevant coexisting attractors. The method is applied to a mechanical system affected by dry friction in which three steady states, two stable and one of saddle-type, exist. In the second part of the paper the evolution of the three steady states is followed as a parameter is varied. It is shown how standard bifurcations and non-smooth bifurcations can interact; in particular an example described in the paper shows that adding-sliding bifurcations may be required before fold bifurcations can take place.

References

- Barreiro, A., Aracil, J., Pagano, D.: Detection of attraction domains of nonlinear systems using bifurcation analysis and Lyapunov functions. *Int. J. Control* **75**, 314–327 (2002)
- Colombo, A., Galvanetto, U.: Stable manifolds of saddles in piecewise smooth systems. *CMES* **53**, 235–254 (2009)

- Cruck, E., Moitie, R., Seube, N.: Estimation of basins of attraction for uncertain systems with affine and Lipschitz dynamics. *Dyn. Control* **11**, 211–227 (2001)
- Di Bernardo, M., Budd, C.J., Champneys, A.R., Kowalzyk, P.: *Piecewise-Smooth Dynamical Systems: Theory and Applications*. Springer, New York (2007)
- Galvanetto, U.: Nonlinear dynamics of multiple friction oscillators. *Comp. Method Appl. Mech. Eng.* **178**(3–4), 291–306 (1999)
- Galvanetto, U.: Numerical computation of Lyapunov exponents in discontinuous maps implicitly defined. *Comput. Phys. Commun.* **131**, 1–9 (2000)
- Galvanetto, U.: Computation of the separatrix of basins of attraction in a non-smooth dynamical system. *Phys. D* **237**, 2263–2271 (2008)
- Hsu, C.S.: *Cell-to-cell mapping: a method of global analysis for nonlinear systems*. Springer, New York (1987)
- Krauskopf, B., Osinga, H.M., Doedel, E.J., Henderson, M.E., Guckenheimer, J., Vladimirovsky, A., Dellnitz, M., Junge, O.: A survey of methods for computing (un)stable manifolds of vector fields. *Int. J. Bifurc. Chaos* **14**, 763–791 (2005)
- Merillas, I.: Modeling and numerical study of nonsmooth dynamical systems. Ph.D. thesis, Dept. Matematica Aplicada IV, Universitat Politècnica de Catalunya (2006)
- Oestreich, M., Hinrichs, N., Popp, K.: Bifurcation and stability analysis for a non-smooth friction oscillator. *Arch. Appl. Mech.* **66**, 301–314 (1996)
- Parker, T.S., Chua, L.O.: *Practical Numerical Algorithms for Chaotic Systems*. Springer, Berlin (1989)
- Soliman, M.S., Thompson, J.M.T.: Integrity measures quantifying the erosion of smooth fractal basins of attraction. *J. Sound Vib.* **135**, 453–475 (1989)
- Thompson, J.M.T., Soliman, M.S.: Fractal control boundaries of driven oscillators and their relevance to safe engineering design. *Proc. R. Soc. Lond. A* **428**, 1–13 (1990)

IUTAM Symposium on Nonlinear Dynamics for Advanced
Technologies and Engineering Design

Proceedings of the IUTAM Symposium on Nonlinear
Dynamics for Advanced Technologies and Engineering
Design, held Aberdeen, UK, 27-30 July 2010

Wiercigroch, M.; Rega, G. (Eds.)

2013, XII, 454 p., Hardcover

ISBN: 978-94-007-5741-7